

We thank F. J. Gilman and Y.-S. Tsai for useful discussions, and acknowledge the support of the Deutsche Forschungsgemeinschaft, the Laboratori Nazionali di Frascati dell'Istituto Nazionale di Fisica Nucleare, and the Swiss National Science Foundation. This work was supported primarily by the U. S. Department of Energy.

¹R. Brandelik *et al.* [Phys. Lett. **73B**, 109 (1978)] give the τ mass as 1.807 ± 0.020 GeV/ c^2 .

²M. L. Perl *et al.*, Phys. Rev. Lett. **35**, 1489 (1975); M. L. Perl, in *Proceedings of the 1977 International Symposium on Lepton and Photon Interactions at High Energies*, edited by F. Gutbrod (Deutsches Elektronen-Synchrotron, Hamburg, Germany, 1977); G. Flüge, in *Proceedings of the Fifth International Conference on Meson Spectroscopy*, Boston, Massachusetts, 29–30 April, 1977 (to be published).

³A. Barbaro-Galtieri *et al.*, Phys. Rev. Lett. **39**, 1058 (1977); A. Barbaro-Galtieri, in *Proceedings of the 1977 International Symposium on Lepton and Photon Interactions at High Energies*, edited by F. Gutbrod (Deutsches Elektronen-Synchrotron, Hamburg, Germany, 1977); G. Knies, *ibid.*; E. Lohrmann, *ibid.*; M. L. Perl, *ibid.*; H. F. W. Sadrozinski, *ibid.*; S. Yamada, *ibid.*

⁴G. Alexander *et al.*, Phys. Lett. **73B**, 99 (1978).

⁵J. J. Sakurai, in *Proceedings of the 1975 International Symposium on Lepton and Photon Interactions at High*

Energies, edited by W. T. Kirk (Stanford Linear Accelerator Center, Stanford, Calif., 1976), p. 353; H. B. Thacker and J. J. Sakurai, Phys. Lett. **36B**, 103 (1971); Y.-S. Tsai, Phys. Rev. D **4**, 2821 (1971); Y.-S. Tsai, private communication.

⁶A recent review of the status of the A_1 can be found in S. M. Flatté, in *Particles on Fields—1977*, edited by G. H. Thomas, A. B. Wicklund, and P. Schreiner (American Institute of Physics, New York, to be published).

⁷G. J. Feldman *et al.*, Phys. Rev. Lett. **38**, 117 (1977).

⁸Neutron Physics Division, Oak Ridge National Laboratory Report No. CCC-178 (unpublished).

⁹The time-of-flight system is discussed in I. Peruzzi *et al.*, SLAC Report No. SLAC-PUB-2067, 1977 (to be published). The K_s^0 identification is described in V. Lüth *et al.*, Phys. Lett. **70B**, 120 (1977).

¹⁰We estimate the muon-momentum spectrum from charm decays by correcting the muon spectrum observed in multiparticle events from Ref. 7 for contamination from τ decays.

¹¹F. J. Gilman and D. H. Miller, SLAC Report No. SLAC-PUB-2046, 1977 (to be published).

¹²The A_1 interpretation has been discussed by J.-L. Basdevant and E. L. Berger, Phys. Rev. Lett. **40**, 994 (1978).

¹³We assume $d\Gamma/dm \propto m(m_\tau^2 - m^2)^2(m_\tau^2 + 2m^2)$ modified by a threshold factor.

¹⁴To evaluate the branching ratios, we have used the calculated cross section for the production of a point-like, spin- $\frac{1}{2}$ particle; the branching ratio $B(\tau \rightarrow \mu\nu\bar{\nu}) = 0.18$, the integrated luminosity (20 pb^{-1}), and the experimental acceptance as determined with Monte Carlo techniques.

Heavy-Ion Fusion Based on the Proximity Potential and One-Body Friction

J. R. Birkelund and J. R. Huizenga

*Departments of Chemistry and Physics, and Nuclear Structure Research Laboratory,
University of Rochester, Rochester, New York 14627*

and

J. N. De and D. Sperber

Department of Physics, Rensselaer Polytechnic Institute, Troy, New York 12180

(Received 21 February 1978)

A simple dynamical model is shown to reproduce heavy-ion fusion excitation functions over a wide mass and energy range. The trajectory calculations employ the proximity nuclear potential and the proximity one-body nuclear friction. The importance of tangential friction in determining the magnitude and shape of the fusion excitation functions at higher energies is discussed.

The measurement of heavy-ion fusion excitation functions offers the possibility of insight into the form of the internuclear conservative force, the magnitude and mechanisms of nuclear friction, and the limits of rotational stability of

heavy nuclei. Analyses of experimental fusion excitation functions on the basis of simple friction-free models have already been reported.^{1,2} These friction-free models assume that a sufficient condition for the fusion of target and pro-

jectile is either that a conservative potential barrier is crossed, or that a critical separation distance is reached.

The well-known damped-reaction process³ gives strong evidence for friction. Hence, dynamical models of fusion including friction have been suggested^{4,5} and some classical trajectory analyses of experimental fusion cross sections at particular energies have been reported.^{5,6} In this Letter we propose a simple dynamical model that gives good agreement with experimental fusion excitation functions over a wide range in energy and mass number. The present trajectory calculations employ the proximity nuclear potential⁷ and one-body nuclear friction.⁸ Friction-free analyses have already indicated that the proximity conservative potential is consistent with heavy-ion fusion data^{9,10} at low energies. In the calculations, the one-body friction is divided into tangential and radial friction forces F_T and F_R , respectively, where

$$F_T = -2\pi n_0 \left(\frac{C_T C_P}{C_T + C_P} \right) b \psi(\xi) U_T, \quad (1)$$

$$F_R = -4\pi n_0 \left(\frac{C_T C_P}{C_T + C_P} \right) b \psi(\xi) U_R.$$

The quantities C_T and C_P are the target and projectile matter half-density radii,⁷ b is the surface diffuseness which was taken to be 1 fm, ξ is the surface separation, and U_T and U_R are the tangential and radial components of the relative surface velocity. The dimensionless universal function ψ has been tabulated by Randrup⁸ and n_0 is the bulk flux of nucleons within the nucleus which was taken to be 0.25×10^{-23} MeV sec fm⁻⁴. The Coulomb potential was given by the potential of two sharp, uniform, spherical charge distributions with radii given by the systematics of Myers.¹¹ The maximum asymptotic entrance-channel orbital angular momentum, l_f , for a trajectory leading to fusion was determined for each system as a function of bombarding energy.¹² The fusion cross section was then determined by use of a sharp-cutoff expression.

The results of the comparison of theoretical fusion excitation functions with experimental data¹³⁻²⁰ are shown for four representative reactions in Figs. 1-4. In the figures the fusion cross section σ_f is plotted versus $1/E_{c.m.}$. Two theoretical curves are shown for each reaction. The dashed curves are theoretical excitation functions based on the proximity nuclear potential without friction. This calculation assumes that

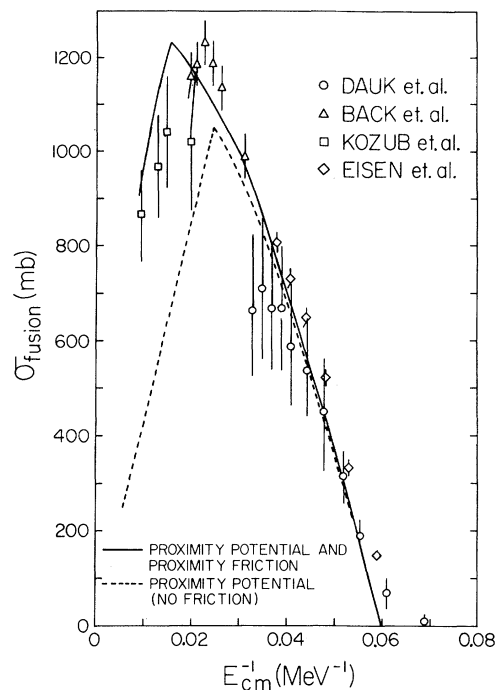


FIG. 1. The fusion cross section σ_{fusion} vs $1/E_{c.m.}$ for the $^{27}\text{Al} + ^{16}\text{O}$ reaction (Refs. 13-16). The data of Refs. 14-16 are based on evaporation-residue measurements and the data of Ref. 13 are based on γ -ray measurements.

a sufficient condition for fusion of a trajectory with any impact parameter is that a pocket, or local minimum, exists in the effective potential, consisting of nuclear, Coulomb, and centrifugal terms, and that the bombarding energy is high enough for the system to cross the outer barrier of the potential pocket. As can be seen from Figs. 1-4, the friction-free model reproduces the experimental data quite well at low energies for all the systems shown. However, at high energies the calculated fusion cross sections decrease more rapidly than the data as the energy is increased. The drop in the fusion cross section at high energies for the friction-free model occurs because the highest value of orbital angular momentum, l_p , for which a pocket exists in the effective potential is fixed independently of bombarding energy. Thus, at high energies the friction-free excitation function decreases as $\pi \lambda^2 l_p^2$.

The solid curves in Figs. 1-4 are the results of full trajectory calculations. At low energies the differences between friction-free excitation functions and those based on the present model are small. This behavior occurs because most of the reaction cross section goes to the fusion

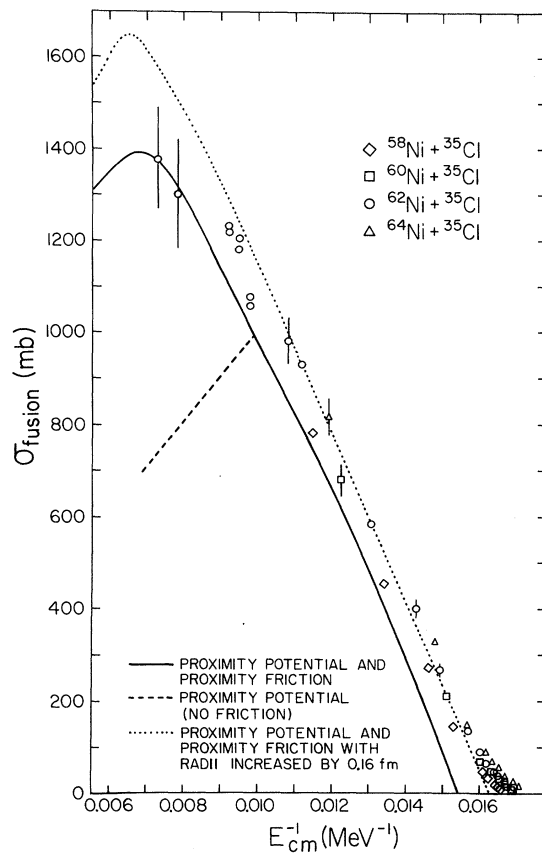


FIG. 2. The fusion cross section σ_{fusion} vs $1/E_{\text{c.m.}}$ for four isotopes of the Ni + ^{35}Cl reaction (Refs. 17 and 18). The experimental fusion cross sections are obtained by summing the evaporation residue and fission cross sections. Fission contributes from 5% at 102 MeV (c.m.) to 26% at 137.4 MeV. The theoretical lines are for the $^{62}\text{Ni} + ^{35}\text{Cl}$ reaction. The theoretical cross sections have maxima at 147 (solid line) and 154 (dotted line) MeV, respectively.

reaction at low energies for the systems shown. Thus, for the trajectory with angular momentum l_f , the relative velocity of the ions within the range of the nuclear friction is almost entirely tangential. Hence, tangential friction is the dominant cause of energy loss along the trajectory in contrast to one of the earlier models.⁵ Energy loss alone is expected to reduce the fusion cross section by reducing the energy below the barrier height for the trajectory with $l = l_f$. However, tangential friction causes a transfer of angular momentum from orbital angular momentum to intrinsic spin of the two nuclei, thus lowering the barrier by reducing the centrifugal potential. At the lower energies these two effects, energy loss and barrier reduction, compensate each other and together have little effect on the fusion cross sec-

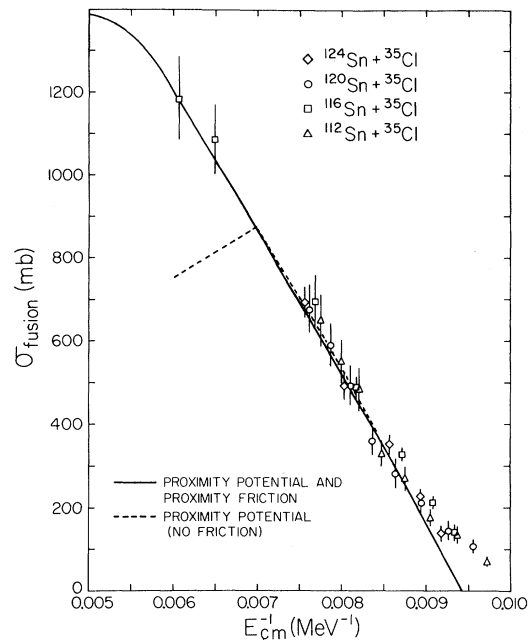


FIG. 3. Similar to Fig. 2 except for four isotopes of the Sn + ^{35}Cl reaction (Refs. 17-19). Fission contributes from 8% at 122 MeV (c.m.) to 50% at 165 MeV. The theoretical lines are for the $^{116}\text{Sn} + ^{35}\text{Cl}$ reaction. The theoretical cross section has a maximum at 192 MeV.

tion. Hence, at low energies the friction-free and dynamical models lead to similar excitation functions.

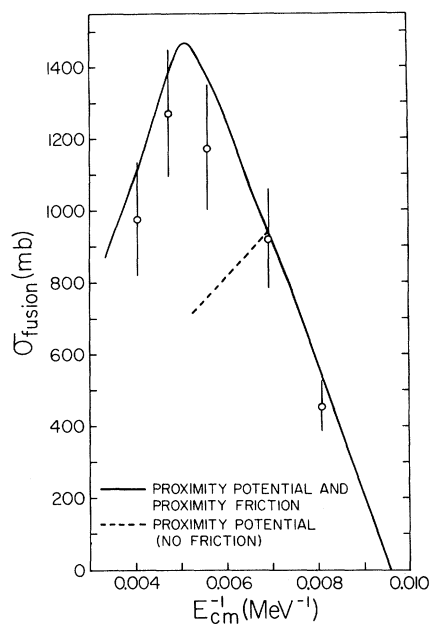


FIG. 4. Similar to Fig. 2 except for the $^{109}\text{Ag} + ^{40}\text{Ar}$ reaction (Ref. 20). Fission contributes from 4% at 123.6 MeV to 53% at 246.5 MeV.

At high energies the two models differ considerably. The dynamical model gives an enhancement of the fusion cross section due to tangential friction. For some trajectories with asymptotic entrance-channel orbital angular momenta greater than l_p , the continuous reduction of orbital angular momentum produced by the tangential friction may bring the trajectory inside a barrier in the instantaneous effective potential at some point during the interaction. If this occurs, then the trajectory will always remain inside a barrier even though further reduction in l may occur. Hence, some trajectories which initially have $l > l_p$ will lead to fusion and thus enhance the fusion cross section over the friction-free value. As the bombarding energy is further increased, the friction is unable to reduce the kinetic energy below the barrier, at radial separations inside the barrier, for an increasing number of impact parameters. Hence the fusion cross section begins to fall as the energy increases, eventually reaching zero at a sufficiently high energy.

The trajectory calculations give fusion excitation functions, for reactions over a wide mass range, which are in excellent agreement with all available experimental data. The decrease in the fusion cross section at the higher energies is also well reproduced by the calculations. However, this result must be viewed with some caution since the calculated angular momentum of the residual nucleus at high energies is close to the maximum possible for a rotating liquid drop.²¹

There is evidence that the one-body friction is too small to explain the energy loss observed in strongly damped collisions.^{3,22} However, considerable orbital angular momentum is dissipated by the one-body tangential friction, resulting in the attainment of the rolling limit for a large number of impact parameters.⁸ Since the fusion cross section is determined ultimately by the number of trajectories leading to capture inside a barrier, the one-body tangential friction may be sufficient to achieve this condition.

In some cases a better agreement between the calculated fusion cross sections and the data may be obtained by a slight increase of the nuclear matter radii over the values suggested by Blocki *et al.*⁷ These increases are generally less than 0.15 fm and are well within the accuracy of the systematics of Myers²³ as used by Blocki *et al.* Such an increase in the matter radii is equivalent to a change in the surface diffuseness used in the proximity potential expression and leads to a small shift of the calculated fusion excitation

functions along the $1/E$ axis in Figs. 1–4. An example of such a shift (corresponding to an increase in the radii of 0.16 fm) is shown by the dotted line in Fig. 2 for the $^{62}\text{Ni} + ^{35}\text{Cl}$ reaction. The maximum value of the theoretical fusion cross section increases by 18% when the larger radii are used. The difference between the solid and dotted curves illustrates the uncertainty in the theoretical cross sections due to variations in the input parameters. All the other theoretical results reported in Figs. 1–4, except the dotted curve in Fig. 2, utilize suggested radial⁷ and frictional⁸ parameters.

This work was supported in part by the U. S. Department of Energy and in part by the National Science Foundation.

¹H. H. Gutbrod, W. G. Winn, and M. Blann, Nucl. Phys. **A213**, 267 (1973).

²D. Glas and U. Mosel, Nucl. Phys. **A237**, 429 (1975).

³W. U. Schröder and J. R. Huizenga, Annu. Rev. Nucl. Sci. **27**, 465 (1977).

⁴J. P. Bondorf, M. I. Sobel, and D. Sperber, Phys. Rep. **15C**, 83 (1974); E. Seglie, D. Sperber, and A. Sherman, Phys. Rev. C **11**, 1227 (1975).

⁵D. H. E. Gross and H. Kalinowski, Phys. Lett. **48B**, 302 (1974).

⁶J. N. De, D. H. E. Gross, and H. Kalinowski, Z. Phys. **A277**, 385 (1976).

⁷J. Blocki, J. Randrup, W. J. Swiatecki, and C. F. Tsang, Ann. Phys. (N.Y.) **105**, 427 (1977).

⁸J. Randrup, NORDITA Report No. 77/36, 1977 (unpublished).

⁹R. Bass, Phys. Rev. Lett. **39**, 265 (1977).

¹⁰J. R. Birkelund and J. R. Huizenga, Phys. Rev. C **17**, 126 (1978).

¹¹W. D. Myers, Phys. Lett. **30B**, 451 (1969).

¹²J. R. Birkelund and J. R. Huizenga, in Proceedings of the Symposium on Heavy-Ion Elastic Scattering, Rochester, N. Y., 1977 (unpublished).

¹³J. Dauk, K. P. Lieb, and A. M. Kleinfeld, Nucl. Phys. **A241**, 170 (1975).

¹⁴B. B. Back, R. B. Betts, C. Gaarde, J. S. Larsen, E. Michelsen, and Tai Kuong-Hsi, Nucl. Phys. **A285**, 317 (1977).

¹⁵R. L. Kozub, N. H. Lu, J. M. Miller, D. Logan, T. W. Debiak, and L. Kowalski, Phys. Rev. C **11**, 1497 (1975).

¹⁶Y. Eisen, I. Tserruya, Y. Eyal, Z. Fraenkel, and M. Hillman, Nucl. Phys. **A241**, 459 (1977).

¹⁷W. Scobel, H. H. Gutbrod, M. Blann, and A. Mignerey, Phys. Rev. C **14**, 1808 (1976).

¹⁸P. David, J. Bisplinghoff, M. Blann, T. Mayer-Kuckuk, and A. Mignerey, Nucl. Phys. **A287**, 179 (1977).

¹⁹B. Sikora, W. Scobel, M. Beckerman, M. Blann, and L. Tubbs, Bull. Am. Phys. Soc. **22**, 1019 (1977).

²⁰H. C. Britt, B. H. Erkill, R. H. Stokes, H. H. Gut-

brod, F. Plasil, R. L. Ferguson, and M. Blann, Phys. Rev. C **13**, 1483 (1976).

²¹S. Cohen, F. Plasil, and W. J. Swiatecki, Ann. Phys. (N.Y.) **82**, 557 (1974).

²²W. U. Schröder, J. R. Huizenga, J. R. Birkelund, K. L. Wolf, and V. E. Viola, Phys. Lett. **71B**, 283 (1977).

²³W. D. Myers, Nucl. Phys. **A204**, 465 (1973).

Observation of 12^- Magnetic Spin States in ^{208}Pb

J. Lichtenstadt, J. Heisenberg, C. N. Papanicolas, and C. P. Sargent

Bates Linear Accelerator Center, Massachusetts Institute of Technology, Cambridge, Massachusetts 02139

and

A. N. Courtemanche and J. S. McCarthy

University of Virginia, Charlottesville, Virginia 22901

(Received 16 February 1978)

States at 6.42-, 6.75-, and 7.06-MeV excitation have been observed in electron scattering on ^{208}Pb . The transverse character of the excitation cross section has been established. The states have been interpreted as the $\nu(i_{13/2}^{-1}j_{15/2})_{12^-,14^-}$ and the $\pi(h_{11/2}^{-1}i_{13/2})_{12^-}$ single-particle hole excitations of the ^{208}Pb ground state, on the basis of the measured momentum-transfer dependence and the magnitude of the cross section.

The nuclear structure of ^{208}Pb has been previously studied by means of inelastic electron scattering.¹ These experiments did not have the necessary high resolution for resolving most of the inelastic excited states. The high resolution available at the Massachusetts Institute of Technology Bates Linear Accelerator allowed the extraction of form factors for more than 25 excited states of ^{208}Pb .² In this Letter we want to report the results for three levels at 6.42, 6.75, and 7.06 MeV, which we believe to be high-spin levels of $J^\pi = 12^-, 14^-,$ and 12^- , respectively, excited via $M12$ and $M14$ transitions.

The experiment was done with incident electron energies of 50 to 335 MeV, detecting the electrons scattered at 90° from enriched ^{208}Pb metallic foils of 30 and 60 mg/cm² thickness. The experiment covered a range of the momentum transfer of $0.4 \leq q \leq 2.4 \text{ fm}^{-1}$. The scattered electrons were analyzed with the high-resolution energy-loss spectrometer.³ The typical energy resolution in this experiment was 40–50 keV. An additional measurement was done at 160° and 200-MeV incident electron energy on an 18-mg/cm² target to ensure the transverse nature of the excitation. A typical spectrum of the scattered inelastic electrons is shown in Fig. 1.

The incident electron energy for each run was obtained from the spectrometer field, measured with a NMR probe, and from the position of the elastic peak in the focal plane and the effective length and dispersion of the spectrometer. To

calibrate the effective length of the spectrometer, we measured at several energies the recoil difference between ^9Be and ^{16}O on a BeO target. The spectrometer dispersion was determined by well-known excitation energies of states in ^{16}O , ^{12}C , ^9Be , and ^{208}Pb .

To extract the cross section we used a line-shape fitting code in which an almost Gaussian shape is folded with the effects of Landau straggling, bremsstrahlung, and Schwinger radiation emission. The line-shape fit to the data is shown in Fig. 1. Cross sections were normalized to the elastic ^{208}Pb cross section, calculated with a phase-shift code from the best fit to all available (e, e') data and muonic x-ray transitions.⁴

The inelastic cross section is given in Born approximation by

$$\frac{d\sigma}{d\Omega} = \left(\frac{d\sigma}{d\Omega} \right)_{\text{Mott}} \{ |F_{\text{long}}(q)|^2 + [1 + \tan^2(\frac{1}{2}\theta)] |F_{\text{trans}}(q)|^2 \}, \quad (1)$$

where F_{long} and F_{trans} are the longitudinal and transverse form factors, respectively. The effects of the distortion of the electron wave are taken into account by plotting in Fig. 2 the data at effective momentum transfer $q_{\text{eff}} = q(1 + 1.33Z\alpha/EA^{1/3})$, (where E is the electron incident energy, and Z and A are the atomic number and the mass, respectively) instead of using the distorted-wave Born approximation. This procedure, for high multipolarity, is a good description of the scat-